The Journal of Chemical Physics

Effects of Zn^{2+} and Ga^{3+} doping on the quantum yield of cluster-derived InP quantum dots

Cite as: J. Chem. Phys. **151**, 194702 (2019); https://doi.org/10.1063/1.5126971
Submitted: 09 September 2019 • Accepted: 28 October 2019 • Published Online: 19 November 2019

Max R. Friedfeld, Jennifer L. Stein, Dane A. Johnson, et al.

AIP Publishing

The Journal of Chemical Physics ARTICLE scitation.org/journal/jcp

Effects of Zn^{2+} and Ga^{3+} doping on the quantum yield of cluster-derived InP quantum dots

Cite as: J. Chem. Phys. 151, 194702 (2019); doi: 10.1063/1.5126971
Submitted: 9 September 2019 • Accepted: 28 October 2019 •
Published Online: 19 November 2019

Max R. Friedfeld,[1,a] Jennifer L. Stein,[1,a] Dane A. Johnson,[1] Nayon Park,[1] Nicholas A. Henry,[1] Michael J. Enright,[1] David Mocatta,[2] and Brandi M. Cossairt[1,b]

AFFILIATIONS

[1] Department of Chemistry, University of Washington, Box 351700, Seattle, Washington 98195-1700, USA
[2] Nanomaterials Group, Performance Materials, Merck Group, Box 39082, 9139002 Jerusalem, Israel

Note: This paper is part of the JCP Special Topic on Colloidal Quantum Dots.
[a] **Contributions:** M. R. Friedfeld and J. L. Stein contributed equally to this work.
[b] **Email:** cossairt@uw.edu

ABSTRACT

As the commercial display market grows, the demand for low-toxicity, highly emissive, and size-tunable semiconducting nanoparticles has increased. Indium phosphide quantum dots represent a promising solution to these challenges; unfortunately, they typically suffer from low inherent emissivity resulting from charge carrier trapping. Strategies to improve the emissive characteristics of indium phosphide often involve zinc incorporation into or onto the core itself and the fabrication of core/shell heterostructures. InP clusters are high fidelity platforms for studying processes such as cation exchange and surface doping with exogenous ions since these clusters are used as single-source precursors for quantum dot synthesis. Here, we examined the incorporation of zinc and gallium ions in InP clusters and the use of the resultant doped clusters as single-source precursors to emissive heterostructured nanoparticles. Zinc ions were observed to readily react with InP clusters, resulting in partial cation exchange, whereas gallium resisted cluster incorporation. Zinc-doped clusters effectively converted to emissive nanoparticles, with quantum yields strongly correlated with zinc content. On the other hand, gallium-doped clusters failed to demonstrate improvements in quantum dot emission. These results indicate stark differences in the mechanisms associated with aliovalent and isovalent doping and provide insight into the use of doped clusters to make emissive quantum dots.

I. INTRODUCTION

The release of the Kindle Fire HDX tablet in 2013 marked the introduction of the use of quantum dots (QDs) in commercial displays. Samsung then commercialized the first cadmium-free quantum dot film-based display in 2015. Since then, the display industry has steadily embraced quantum dot technologies, with dozens of products now available from many display manufacturers. In the future, a variety of new implementations of quantum dots are poised to change the way we view the world through screens.[1,2]

Given the current metrics for commercial-grade quantum dots, cadmium-free QD materials based on indium phosphide still lag behind the champion CdSe materials in terms of quantum yield and emission linewidth, reducing the practical color gamut coverage provided by these less-toxic materials. One of the principal approaches to further improve the properties of InP quantum dots involves increasing the complexity of the material itself through core alloying and the formation of gradient core/shell and core/shell/shell materials. Over the past decade, many different methods to make high photoluminescence quantum yield (PLQY) InP QDs have been developed which rely on optimized shell growth. Thick ZnSe shells have been demonstrated to thermodynamically isolate charge carriers and increase InP PLQY above 40%.[3] InP/ZnSe/ZnS core/shell/shell nanoparticles have recently been reported to facilitate high PLQY (>70%) by lowering lattice strain and improving passivation of the InP core.[4,5] The highest reported InP quantum yield relied on this strategy to achieve 95% PLQY with highly designed InP/ZnSe/ZnS QDs.[6]

In numerous reports, including several of the above preparations of core/shell quantum dots, the synthesis of InP cores is performed in the presence of a Zn^{2+} source.[7–12] The addition of Zn^{2+} has been demonstrated to improve quantum yields and result in narrower size distributions when compared to syntheses that do not incorporate Zn^{2+}. The mechanism and origin of this phenomenon is not well understood, but it is thought that zinc is involved in the nucleation both as a gating precursor to moderate conversion kinetics and also as an aliovalent Z-type ligand at the InP surface, altering growth and modulating the lattice constant between the core and shell layers of the final heterostructures.[12] Building off of these methodologies, isovalent Ga^{3+} has recently gained traction as a potential ingredient to modulate InP nucleation, growth, and photophysics. For example, InP/GaP/ZnSe systems have been demonstrated to achieve up to 85% PLQY.[13,14] In another study, using different gallium precursors in the synthesis of Ga-doped InP imparted distinct reactivity and optical properties on the final QD cores.[15] Cation exchange was demonstrated in a Zn-doped InP system, which, when exposed to gallium oleate, resulted specifically in Ga-for-Zn cation exchange, resulting in >70% PLQY.[16]

To date, studies on zinc and gallium incorporation into InP QDs have been approached from a purely empirical standpoint with little attention to the creation of new, generalizable principles to move the field forward. Much of this research has focused on the synthesis of zinc and gallium alloyed InP QDs from molecular precursors, which is limited by the inherent reactivity of the precursors themselves and fails to provide control over the extent of alloying. Instead, InP clusters present a stoichiometrically precise platform to introduce dopant ions in a controlled and precise fashion. Research in our lab has focused on the synthesis and electronic structure assignment of a kinetically stable InP cluster, $In_{37}P_{20}X_{51}$ (X = carboxylate), and elucidation of the mechanism by which this cluster converts to larger InP QDs.[17–19] Previously, we have shown that the InP cluster reacts with cadmium carboxylate to undergo cation exchange, eventually resulting in the full conversion of the InP cluster to Cd_3P_2 clusters.[20] Similarly, we hypothesized that the InP crystal lattice could be modified more generally via cation doping processes to furnish doped clusters with new properties. These new doped clusters could then be used as single-source precursors in the synthesis of new InP core/shell QDs, whose electronic properties could potentially be determined by the concentration and/or location of the dopant ions in the treated cluster material. In this report, we will discuss the incorporation of aliovalent Zn^{2+} and isovalent Ga^{3+} into the InP cluster and the role these ions have on the photoluminescent properties of core/shell QDs derived from these clusters.

II. RESULTS AND DISCUSSION

A. Cluster cation doping with Zn and Ga

Our efforts to dope $In_{37}P_{20}(MA)_{51}$ [MA = myristate, $^{-}O_2C(CH_2)_{12}CH_3$] began with treating the cluster with different zinc precursors. Zinc myristate proved to be relatively unreactive toward cation exchange from room temperature to 100 °C, resulting in no zinc incorporation as evidenced by UV-Vis and ^{31}P NMR spectroscopy (see the supplementary material, Fig. S1), whereas treatment with Et_2Zn led to cluster inhomogeneity and decomposition (see the supplementary material, Fig. S2). We next sought to examine the mixed alkyl, carboxylate zinc precursor $Zn_5(Et)_4(OAc)_6$ which has previously been demonstrated to serve as a reactive precursor in the synthesis of zinc phosphide quantum dots.[21,22] Treatment of $In_{37}P_{20}(MA)_{51}$ with 4–24 M equivalents of Zn^{2+} using $Zn_5(Et)_4(OAc)_6$ for 72 h at room temperature resulted in slight changes in the UV-Vis spectrum and the powder XRD pattern [Figs. 1(a) and 1(c)]. The photoluminescence spectra of clusters exposed to these lower [Zn^{2+}] displayed a broad emissive feature that is distinct from pure InP cluster emission, providing an indication of the extent of zinc doping. Phosphorous NMR spectroscopy is an effective way of interrogating the internal cluster structure, as the InP cluster exhibits 11 distinct ^{31}P resonances in the range of −180 to −250 ppm, corresponding to different phosphorus chemical environments within the InP core. Cation doping at the cluster surface or within the core lattice should lead to changes in the ^{31}P NMR spectrum. The ^{31}P NMR spectrum [Fig. 1(e)] of these products shows significant broadening of the primary cluster resonances and slight upfield shifts, while the powder XRD patterns [Fig. 1(c)] indicate little change in the crystalline domains. This suggests that the structure of the original InP cluster has been altered in a non-site-selective manner while keeping the low-symmetry phosphide sublattice relatively intact similar to our earlier observations of the early stages of cadmium doping into the InP cluster.[20] As determined by inductively coupled plasma-optical emission spectroscopy (ICP-OES), the amount of zinc present in the final material relative to indium increases as the initial [Zn^{2+}] increases, eventually reaching a maximum of 1.3:1 Zn:In (see Fig. 2 and the supplementary material, Table S1, Fig. S3). The changes in the core structure upon zinc incorporation are also evident in the matrix-assisted laser desorption/ionization-time of flight (MALDI-TOF) mass spectra of the doped clusters, where a shift to lower m/z ratios and broadening is observed upon increased zinc incorporation (see the supplementary material, Figs. S4 and S5).

Achieving cation doping with gallium proved more challenging. Precursor development for accessing gallium-based nanomaterials is limited compared to zinc. Common gallium precursors used in quantum dot and vapor-phase deposition synthesis include gallium acetylacetonate, trimethylgallium, and tris(dimethylamido)gallium. No gallium analog to the mixed alkyl/carboxylate zinc cluster exists, though gallium dimers of the form $[Ga(R)_2X]_2$ (R = alkyl, X = carboxylate) have been reported.[23,24] Examination of $[Ga(CH_3)_2(MA)]_2$ as a gallium precursor showed low gallium incorporation into the cluster as evidenced by ICP-OES (less than 10% Ga, see the supplementary material, Table S2). However, the ^{31}P NMR spectrum indicated heterogeneous gallium incorporation and cluster degradation (see the supplementary material, Fig. S6). Consequently, this precursor was not pursued further. Instead, gallium acetate, $Ga(OAc)_3$, was chosen as the most suitable gallium precursor due to its synthetic accessibility and ready analogy to the indium carboxylate precursors common in InP synthesis.[25] Stirring a toluene solution of $In_{37}P_{20}(MA)_{51}$ with increasing equivalents of $Ga(OAc)_3$ at room temperature for 48 h followed by cluster purification resulted in UV-Vis absorbance spectra and powder XRD patterns that resemble an undoped cluster material [Figs. 1(b) and 1(d)]. However, the ^{31}P NMR spectra [Fig. 1(f), see the supplementary material, Figs. S7 and S8] show both new resonances attributed to gallium-doped clusters and subtle shifts in

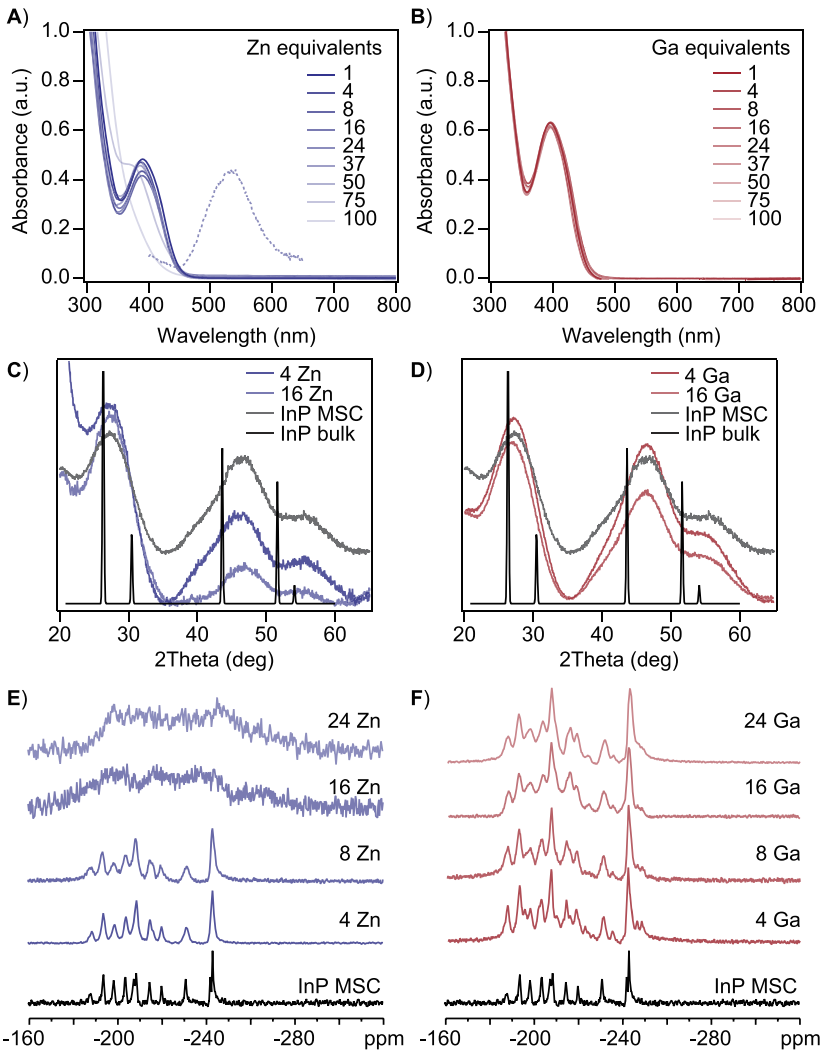

FIG. 1. Cluster doping with zinc and gallium precursors. (a) UV-Vis and PL spectra for Zn-doped InP clusters. (b) UV-Vis spectra for Ga-doped InP clusters. (c) Powder XRD patterns of Zn-doped InP clusters. (d) Powder XRD patterns of Ga-doped InP clusters. (e) ^{31}P NMR spectra of Zn-doped InP clusters. (f) ^{31}P NMR spectra of Ga-doped InP clusters.

the phosphide core resonances of the starting pure-phase cluster, suggesting gallium coordination at the cluster surface. After the cluster has been treated with approximately 16 equivalents of gallium, no further change is observed in the ^{31}P NMR spectrum, indicating saturation and no further gallium incorporation. In fact, heating a mixture of InP cluster and 100 eq. $Ga(OAc)_3$ at 80 °C for 24 h furnished a ^{31}P NMR spectrum very similar to that of other, more mild doping conditions (see the supplementary material, Fig. S9). This gallium doping saturation is corroborated by the elemental analysis of the treated cluster samples (Fig. 2), where the Ga:In ratio saturates at approximately 0.07 upon adding 24 equivalents of $Ga(OAc)_3$ to the cluster (see the supplementary material, Table S1), suggesting incorporation of on average 2–3 equivalents of Ga^{3+} into the resultant clusters.

These results demonstrate how charge and size differences between Zn^{2+} and Ga^{3+} impact the ability of the dopant metals to enter the InP cluster crystal lattice. While both dopants are smaller than In^{3+} (80 pm), the effective ionic radius of Zn^{2+} (74 pm) matches more closely with that of Ga^{3+} (62 pm).[26] A similar trend is observed in the chemical hardness, η, where Zn^{2+} (10.88) is more closely matched with In^{3+} (13) compared to Ga^{3+} (17).[27] The mechanism of Zn^{2+} cation exchange likely follows that of Cd^{2+} wherein an initial topotactic surface exchange occurs. In the case of these divalent ions, exchange into the core requires either charge compensation at the surface (i.e., loss of carboxylate) at modest dopant levels or eventual expulsion of phosphorus anions and formation of obligate phosphorus vacancies at high concentrations. This appears to occur in a nondestructive manner in the case of Cd^{2+} because of its similar size (95 pm) and hardness (10.29) when compared to In^{3+},[20] but in the case of Zn^{2+}, the smaller ionic radius precludes cation exchange into the core without at least partial cluster dissolution. In the case of isovalent Ga^{3+}, the lack of obligate anion loss and vacancy formation eliminates possible mechanisms for relieving strain induced upon incorporation of this smaller cation. Therefore, Ga^{3+} is not readily

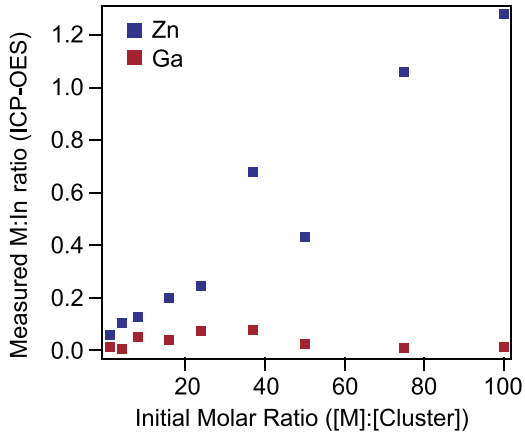

FIG. 2. Elemental analysis (ICP-OES) of clusters after exposure to cation doping conditions.

incorporated beyond the surface. Even exposing the InP cluster to 100 eq. of $Ga(OAc)_3$ at 80 °C for 24 h resulted in minimal incorporation or phosphide lattice dissolution, instead retaining strong interactions between Ga^{3+} and its associated hard acetate ions. Similar charge-balancing effects have been invoked in gallium for zinc aliovalent cation exchange in InP QDs.[16]

To provide a more direct comparison with the zinc-doped clusters, we sought to develop a method for increasing the extent of gallium incorporation as a means to evaluate the effect of gallium content on the resultant QD PLQY. The reaction of InP clusters with 4, 8, and 16 equivalents of [Ga^{3+}] using $[Ga(NMe_2)_3]_2$ in toluene solvent at room temperature resulted in a red-shifting of the primary absorbance feature (see the supplementary material, Fig. S10). It should be noted that this shift is similar to what has been observed upon treatment of InP clusters with primary amine and therefore may be an effect of ligand exchange rather than an indication of cation exchange.[31] The ^{31}P NMR spectra for this series of cation-doped clusters indicated a loss of the characteristic cluster phosphide resonances, and at 8 and 16 equivalents of [Ga^{3+}], a broad feature is observed in the phosphide region. ICP results of purified clusters indicate that, upon exposure to 8 and 16 equivalents of [Ga^{3+}], the resultant materials had an In:Ga ratio of 1:0.24 and 1:0.43, respectively (see the supplementary material, Table S3), a significant increase in gallium content relative to using $Ga(OAc)_3$. Upon exposure to higher concentrations of the gallium amide precursor, a significant decrease in solubility of the cluster was observed, which could be recovered upon addition of equimolar equivalents, relative to [Ga^{3+}], of myristic acid. While it is difficult to determine the extent of cation exchange in this reaction relative to gallium incorporation on the surface, these samples present a useful comparison as gallium-rich precursors for core/shell QDs and were also examined as single-source precursors to core/shell QDs.

B. Conversion of doped clusters to InP core and core/shell QDs

Having demonstrated a strategy to introduce zinc and gallium into the cluster lattice, we next sought to evaluate these modified clusters as single-source precursors for synthesizing high PLQY InP QDs. First, the cluster conversion to doped InP QD cores was examined to determine if dopant concentrations can be maintained upon QD synthesis. The conversion of InP clusters to larger QDs has previously been studied, identifying high temperatures and short reactions times as optimal for producing monodisperse QD samples.[19] In analogy, zinc- and gallium-doped clusters were dissolved in 1 ml 1-octadecene (1-ODE) and rapidly injected into a flask of 1-ODE at 300 °C. The reaction was monitored by UV-Vis and PL spectroscopy, and after 15 min of core growth, the reaction was cooled and the resulting material was purified. With increasing zinc content, the final absorbance feature (Fig. 3) blue-shifted from 580 nm (0 eq. added Zn^{2+}) to a less defined feature at 490 nm (100 eq. added Zn^{2+}). The absorbance features of the two samples with greater than 50 eq. added Zn continued to blue-shift even at room temperature on the day following QD growth, indicating instability of the resultant doped materials.

The trend observed in the absorbance spectra for zinc-doped InP QDs is reflected by the particle sizes measured by transmission electron microscopy (TEM). Representative TEM images of samples treated with initial [Zn^{2+}]:cluster ratios of 1, 4, and 16 indicate particle diameters of 2.6 nm, 2.3 nm, and 2.1 nm (see the supplementary material, Fig. S11). The moderate size differences across this family of zinc-doped InP QDs are consistent with previous reports of zinc-doped InP QDs prepared from mixtures of indium and zinc carboxylates and $P(TMS)_3$,[9,12] wherein the presence of zinc during nucleation serves to moderate the precursor reactivity and results

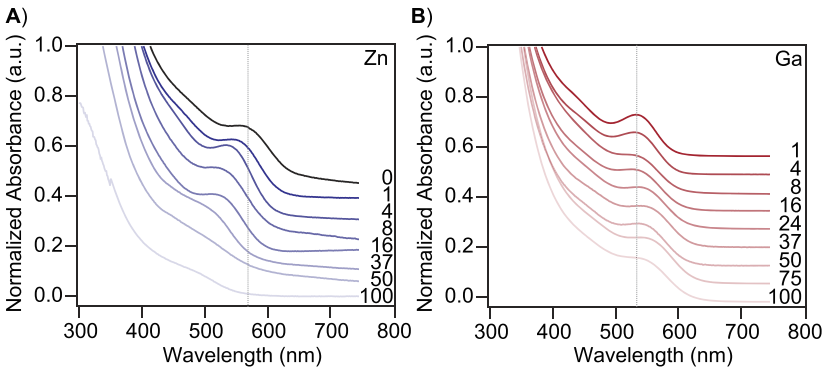

FIG. 3. UV-Vis spectra of zinc-doped (a) and gallium-doped (b) InP QDs. Zinc and gallium equivalents refer to original added concentration during cluster cation doping.

in smaller particles. In a number of imaged samples and corroborated through powder XRD (Fig. S11), the presence of In_2O_3 was observed which is consistent with other reports of Zn-doped InP prepared from molecular precursors of indium and zinc carboxylates and tris(trimethylsilyl)phosphine.[28] At higher [Zn^{2+}]:cluster ratios, a high level of morphological variation is observed, precluding quantitative size measurement. This variation is also observed in the powder XRD patterns at high [Zn^{2+}]:cluster ratios, which are significantly broadened, indicating a loss of crystallinity (see the supplementary material, Fig. S11). The powder XRD patterns of samples treated with initial [Zn^{2+}]:cluster ratios of 1, 4, and 16 do not display peak shifts to higher degrees 2Θ, which would correspond to lattice contraction consistent with homogeneous zinc alloying throughout the crystalline domain. This suggests that zinc doping is heterogeneous and likely limited to the outer layers of the InP QDs.

The PLQY of the doped clusters correlates with the extent of zinc incorporation, increasing from 0.2% for the undoped samples to 19% PLQY for the QDs synthesized from doped clusters using 16 equivalents of [Zn^{2+}] (see the supplementary material, Fig. S12). These PLQYs are comparable to the range reported for zinc-doped InP QDs prepared by a one-pot synthesis from molecular precursors[7,9–11] and with reports of postsynthetic functionalization of InP surfaces with Zn^{2+} as a Z-type ligand.[8,29] The measured Zn:In ratios of these QDs are higher compared to the measured Zn:In ratios of the doped cluster precursors, indicating that higher concentrations of zinc can be incorporated into the QD crystal lattice. It has been posited by Houtepen and co-workers that phosphorus vacancies form to balance the charge as zinc is incorporated, which is consistent with our experimental data.[28]

The gallium-doped clusters are also effective precursors for synthesizing doped InP QDs. Unlike the zinc-doped QDs, gallium-doped QDs exhibit a slight redshift in the absorbance feature compared to the undoped material (see Fig. 3). This suggests that the gallium ions are not accumulating at high concentrations in the crystal lattice and are not contributing significantly to the electronic structure of the QDs, since GaP has a larger bandgap than InP.[30] This is corroborated by the powder XRD patterns, which indicate predominantly zinc blende InP (see Fig. S13), and the ICP-OES analysis, which indicates similar Ga:In ratios as were found in the doped cluster samples (see the supplementary material, Table S4). Furthermore, in contrast to the zinc-doped InP QDs, the gallium-doped species exhibited <1% PLQY across the series, similar in nature to undoped InP QDs.

Having demonstrated that zinc and gallium dopants are incorporated into InP QD materials using doped clusters as single-source precursors, we next sought to use these materials as synthons for high PLQY QD materials. Zinc-doped InP QD cores should interface more epitaxially with ZnSe and ZnS shells (having a 7.7% and 3.4% lattice mismatch, respectively, with InP),[7] as the zinc doping should improve the lattice mismatch. We selected a ZnSeS gradient alloy shell to mitigate direct contact between ZnS and InP and to confine the exciton to the core more effectively (via a type 1 core/shell architecture).[7,30] Experimental conditions for shell growth were adapted from a report by Lee and co-workers who were able to synthesize InP/ZnSeS via molecular precursors with PLQYs up to 65% with 70 nm FWHM emission linewidths.[7] Briefly, zinc stearate was added in excess of InP (10:1 Zn:In in the case of undoped cluster samples) at 200 °C, after which a solution of trioctylphosphine selenide (TOPSe) followed by trioctylphosphine sulfide (TOPS) was added. Under these conditions, a ZnSeS shell of approximately 5 monolayers was targeted.[7] After incubation, the temperature was gradually increased (see the supplementary material and Sec. IV for complete details).

The PLQYs of InP/ZnSeS particles with initial [Zn^{2+}]:cluster ratios of 1, 4, 8, and 16 are presented in Fig. 4. There is a direct correlation between increased PLQY and increasing [Zn^{2+}]:cluster ratios during the initial cation doping reaction, where the highest PLQY, 85%, was measured for the sample with an initial [Zn^{2+}]:cluster ratio of 16 compared to 63% ± 6% when using undoped clusters. While the emission linewidths are broad in comparison with other shelling procedures that report linewidths in the range of 40–60 nm, there is a consistent decrease in linewidth from samples with initial [Zn^{2+}] of 0 equivalents (85 nm) to samples with initial [Zn^{2+}] of 16 equivalents (66 nm). This decrease in FWHM is likely a result of increasingly uniform shell deposition.

To investigate whether these results are the effect of increasing zinc doping into clusters or rather just the presence of zinc in the reaction mixtures, we performed a set of experiments in which zinc doping via cation exchange did not occur prior to cluster conversion. In these experiments, InP clusters were briefly (2 h vs 72 h) exposed to 4, 8, and 16 equivalents of [Zn^{2+}]. At this short time interval, doping was not observed in the 2 h samples as evidenced by ^{31}P NMR spectroscopy or UV-Vis/PL spectroscopy.

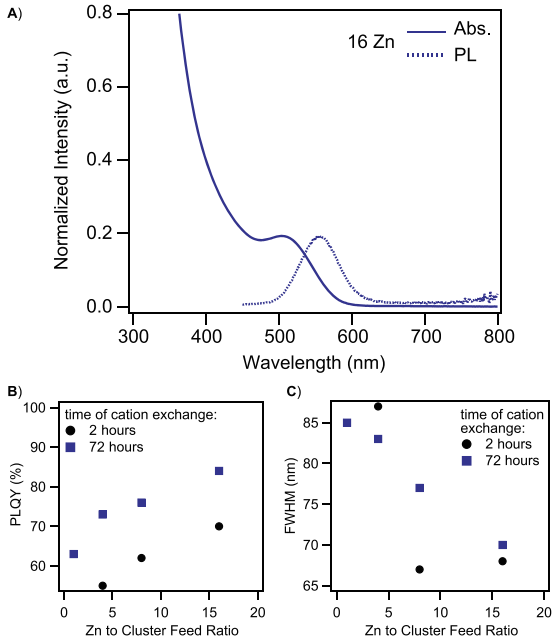

FIG. 4. (a) UV-Vis and PL spectra of the representative zinc-doped InP/ZnSeS sample. Absorbance and photoluminescence spectra are normalized to their respective peak maxima. (b) PLQY vs [Zn^{2+}] to cluster feed ratios for final core/shell QDs with different cation doping times. Photoluminescent peak maxima for the zinc-doped series are 572, 578, 554, and 556 nm for 1, 4, 8, and 16 eq. [Zn^{2+}], respectively. (c) FWHM vs [Zn^{2+}] to cluster feed ratios for final core/shell QDs.

These samples were then converted to InP QDs via hot-injection and subjected to shell growth via analogous conditions. The optical properties of QDs prepared from cation-exchanged clusters (72 h) were significantly different compared to samples that were only briefly exposed to zinc cations (see Fig. 4, purple squares vs black circles), exhibiting universally higher PLQY and comparable FWHM. These results indicate the importance of fully equilibrating zinc into the InP cluster lattice during cation exchange, and the effects that full cation exchange has on subsequent QD core/shell synthesis.

Gallium-doped clusters were next employed as single-source precursors for core/shell QD synthesis using similar reaction conditions. While the levels of gallium doping are lower compared to those of zinc, it was still expected that the presence of gallium might aid in the formation of a more defect-free core/shell interface. This should arise from the smaller ionic radius of gallium acting to contract the overall InP lattice constant and aligning it more closely with ZnSe and ZnS. Subjecting the gallium-doped cluster samples to core/shell QD synthesis furnished InP/ZnSeS materials with PLQYs in the range of 45%–60% (Fig. 5, Figs. S14 and S15). In contrast to the zinc-treated clusters, the cluster samples exposed to higher initial [Ga^{3+}] during cation exchange exhibited a lower PLQY after the shelling procedure as compared to undoped samples. Furthermore,

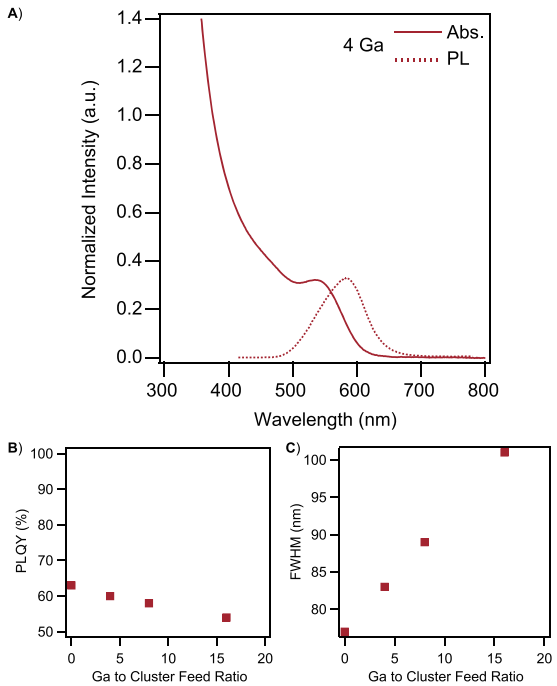

FIG. 5. (a) UV-Vis and PL spectra for representative gallium-doped InP/ZnSeS core/shell QDs synthesized using a [Ga^{3+}] to cluster feed ratio of 4. Absorbance and photoluminescence spectra are normalized to respective peak maxima. (b) PLQY vs [Ga^{3+}] to cluster feed ratios for final core/shell QDs. Photoluminescent peak maxima for the gallium-doped series are 577, 583, 574, and 602 nm for 0, 4, 8, and 16 eq. [Ga^{3+}], respectively. (c) FWHM vs [Ga^{3+}] to cluster feed ratios for final core/shell QDs.

the FWHM of PL emission for the gallium-doped InP/ZnSeS materials increased significantly as the PLQY decreased, indicating that exposing InP clusters to increasing concentrations of $Ga(OAc)_3$ has a deleterious effect on both the PLQY and the FWHM of excitonic emission. We propose that the increased FWHM and decreased PLQY arise from cluster destabilization that arises both from cluster doping and from the exchange of long-chain carboxylate ligands for acetate ligands on the cluster surface. The powder XRD patterns for these core shell materials (Fig. S16) show reflections shifted away from pure zinc blende InP, indicating that the ZnSeS shell has interfaced with the InP core. ICP results (see the supplementary material, Table S5) demonstrate that the gallium concentration relative to indium in the final core/shell material is similar to the unshelled InP QDs.

Having observed the lower PLQY with the lightly gallium-doped samples, we next sought to evaluate the performance of the gallium-rich samples prepared with $[Ga(NMe_2)_3]_2$. However, using even these gallium-rich materials in the synthesis of InP/ZnSeS in an analogous method as before failed to produce the material with significantly greater PLQY than that obtained from undoped clusters. Instead, PLQY between 58% and 74% was obtained using these gallium-amide-treated samples. This modest increase in PLQY could be attributed to the slightly higher gallium content in these materials (In: Ga ratios up to 1:0.16 as evidenced by ICP analysis, see the supplementary material, Table S6). A further complication with this method arises from the poor stability from these doped clusters due to the presence of the amide ligands. In fact, when using the cluster exposed to 16 eq. [Ga^{3+}] in the absence of stabilizing myristic acid ligands, QD dissolution and decomposition were observed during synthesis, resulting in 15% PLQY in the final material. The presence of myristic acid is helpful in improving the solubility and stability of the clusters without affecting the cluster In:Ga ratios (see the supplementary material, Table S6). These results indicate that even using gallium-rich clusters, no significant increase in PLQY is obtained upon core/shell QD synthesis and that using $[Ga(NMe_2)_3]_2$ to introduce gallium into the cluster presents further complications regarding cluster stability and solubility.

A similar trend in PLQY is observed following the postsynthetic surface-treatment of native, unshelled InP QDs with metal carboxylates. In the previous work, we have shown that treatment of InP QDs with either cadmium carboxylate or zinc carboxylate resulted in significant enhancement in PLQY (increasing from <1% PLQY to 16% for Zn treatment and 30% for Cd treatment).[8] This PLQY enhancement was attributed to passivation of the surface trap states by the metal carboxylate that was facilitated by the high affinity for Cd^{2+} and Zn^{2+} to bind to the surface of the QD. Treating InP QDs with gallium myristate in an analogous manner resulted in a slight blueshift in the absorbance peak yet failed to produce a PLQY enhancement (see the supplementary material, Fig. S17). We hypothesize that this lack of surface passivation and PLQY enhancement arises from low thermodynamic driving forces for gallium binding or cation exchange, which in turn are a function of the smaller size and higher chemical hardness of gallium ions compared to indium and higher obligate ligand (anion) coordination number compared to zinc. This result is consistent with a previous report wherein zinc-free InP QDs resisted gallium cation exchange and gallium incorporation on the InP QD surface failed to improve the PLQY.[16]

III. CONCLUSIONS

We have reported the behavior of InP clusters toward cation doping with Zn^{2+} and Ga^{3+}. The most effective zinc precursor was a mixed alkyl-carboxylate cluster, $Zn_5(Et)_4(OAc)_6$, whereas both $Ga(OAc)_3$ and $[Ga(CH_3)_2(MA)]_2$ displayed similar activity toward cluster doping. Zinc demonstrated efficient doping of the cluster, while gallium proved resistant toward cluster doping. We have attributed this disparity in reactivity to differences in chemical hardness, ionic radii, and valency of Zn^{2+} and Ga^{3+} compared to In^{3+}. These doped cluster samples were then evaluated as precursors for emissive InP/ZnSeS core shell nanomaterials. The zinc-doped samples exhibited improved emissive performance (PLQY and FWHM) compared to undoped samples, achieving 85% PLQY and 70 nm FWHM in the final material after exposing the InP cluster to 16 eq. [Zn^{2+}]. The InP/ZnSeS core shell material using gallium-doped clusters, however, exhibited lower emissive performance even after developing a strategy to obtain higher gallium doping using $[Ga(NMe_2)_3]_2$.

Previous reports have demonstrated a minimal extent of gallium exchange in InP QDs when compared to zinc,[16] similar to what we see here for InP clusters. Taken as a whole, these results suggest that ionic radii, chemical hardness, and valency must be taken into account when designing strategies to chemically elaborate InP QDs. A large discrepancy in ionic radius, for example, can be tolerated in cases of aliovalent doping where strain may be alleviated through anion vacancy formation. Furthermore, the lack of positive impacts on InP emissive properties from gallium doping observed here suggests that isovalent dopants with high chemical hardness and relatively small ionic radii may not be ideal for modulating lattice strain between InP cores and Zn chalcogenide shells in the absence of codopants or engineered defects. New innovations in doping chemistries, shelling strategies, and surface chemistry are still needed to address carrier trapping and interfacial strain to reliably access defect-free InP QDs with optimal emissive properties.

IV. EXPERIMENTAL

All glassware was dried in a 160 °C oven overnight prior to use. All reactions, unless otherwise noted, were run under an inert atmosphere of nitrogen using a glovebox or using standard Schlenk techniques. *Warning: $P(SiMe_3)_3$ is pyrophoric and extremely reactive and should be handled with caution.* Indium acetate (99.99%), myristic acid (99%), gallium nitrate hydrate (99.9%), zinc acetate (99.99%), zinc stearate, acetic anhydride, trioctylphosphine, (97%), sulfur (>99%), selenium (99.99%), and trans-2-[3-(4-tert-Butylphenyl)-2-methyl-2-propenylidene]malononitrile (DCTB) (≥99.0%) were purchased from Sigma-Aldrich Chemical Co. and used without further purification. $[Ga(NMe_2)_3]_2$ (98%) and diethyl zinc (>95%) were purchased from Strem Chemicals and used without further purification. Bio-Beads S-X1 was purchased from Bio-Rad Laboratories. All solvents, including 1-ODE, toluene, pentane, ethyl acetate, and acetonitrile, were purchased from Sigma-Aldrich Chemical Co., dried over CaH_2, distilled, and stored over 4 Å molecular sieves in a nitrogen-filled glovebox. C_6D_6 was purchased from Cambridge Isotope Laboratories and was similarly dried and stored. OmniTrace nitric acid was purchased from EMD Millipore and used without further purification. 18.2 MΩ was collected from an EMD Millipore water purification system. $P(SiMe_3)_3$ was prepared following literature procedures.[32]

^{31}P NMR spectra were collected on a 700 MHz Bruker Advance spectrometer. UV-Vis spectra were collected on a Cary 5000 spectrophotometer. TEM images were collected on an FEI Tecnai G2 F20 microscope using an ultrathin carbon film on holey carbon grids purchased from Ted Pella, Inc. Powder X-ray diffraction (XRD) patterns were collected with a Bruker D8 Discover with IμS 2-D XRD system. Fluorescence and quantum yield measurements were taken on a Horiba Jobin Yvon FluoroMax-4 fluorescence spectrophotometer with the Quanta-phi integrating sphere accessory. ICP-OES was performed using PerkinElmer Optima 8300. MALDI-TOF mass data were collected on a Bruker Autoflex II instrument using DCTB as the matrix. Cluster samples dispersed in toluene were mixed with toluene solutions of the matrix and spotted on a stainless-steel plate in a glovebox. Desorption and ionization of samples were achieved by irradiation with a pulsed nitrogen laser. Mass spectra were measured with the detector in the linear positive mode with a laser intensity between 5% and 15%. Calibration was performed using external standards ubiquitin I, myoglobin, and cytochrome C. Data were smoothed and fitted in Igor Pro using binomial smoothing algorithms.

A. $Zn_5(O_2CCH_3)_6(CH_2CH_3)_4$ (Zn5) cluster synthesis

$Zn_5(O_2CCH_3)_6(CH_2CH_3)_4$ was synthesized following a literature procedure[21] where zinc acetate (1.107 g, 6.03 mmol) was dissolved in toluene (5 ml) and then diethyl zinc (413 μl, 4.02 mmol) was added dropwise to the stirring solution.[25] The reaction was allowed to complete at room temperature overnight. The toluene was concentrated under vacuum, and then the Zn5 cluster was precipitated with the addition of heptane. The white solid was dried *in vacuo* and confirmed pure by ^1H NMR.

B. $Ga(OAc)_3$ synthesis

Following a literature procedure,[25] gallium nitrate hydrate (5 g) was dissolved in 50 ml acetic anhydride in a 3-neck round bottom flask equipped with a stir bar. The flask was equipped with a distillation apparatus and a mineral oil bubbler. The flask was heated to reflux for 2 h, upon which time orange vapor ceased evolution and a white precipitate had formed. *Caution: this reaction evolves acetic acid and NO_x gases, and care should be taken for proper ventilation and pressure regulation.* The remaining solvent was distilled, and the residual white solid was washed with toluene (10 ml) and ethyl acetate (2 × 10 ml) and dried *in vacuo* to afford a white free-flowing powder. The attenuated total reflection (ATR) spectrum matched the literature report. The hydroscopic white solid was stored in an N_2-filled glovebox.

C. Zn^{2+} doping of InP cluster

Typical titration experiments were conducted by dissolving 40 mg of $In_{37}P_{20}(O_2C_{14}H_{27})_{51}$ in toluene (2 ml) and adding varying equivalents (1, 4, 8, 16, 24, 37, 50, 75, and 100) of [Zn^{2+}] from a stock solution of Zn5 to stir at room temperature. The Zn5 stock solution was prepared by dissolving 54 mg (7×10^{-3} mol) of Zn5 in 2 ml of toluene to make a 0.034M solution. The reaction was monitored by UV-Vis aliquots taken over 2, 20, 48, and 84 h intervals. Reactions to

examine the products of InP MSCs and diethyl zinc or zinc myristate were conducted in a similar fashion either at room temperature or by heating to 50 °C under N_2 on a Schlenk line. Samples were purified by gel permeation chromatography (GPC) by loading the reaction solution directly into a toluene-based column. For the 2 h reaction time samples, clusters were dissolved in 1 ml of ODE rather than toluene to prepare for hot-injection.

D. Ga^{3+} doping of InP cluster

Typical titration experiments were conducted by dissolving 200 mg of $In_{37}P_{20}(O_2C_{14}H_{27})_{51}$ in toluene (2 ml) and adding varying equivalents (1, 4, 8, 16, 24, 37, 50, 75, and 100 equivalents relative to the cluster) of $Ga(OAc)_3$. The reaction mixture was stirred for 48 h with UV-Vis monitoring. The solutions were centrifuged to remove the insoluble material, and the supernatant was purified by GPC by loading into a toluene-based column.

E. Doped InP QD growth

In a typical QD growth reaction, the doped clusters were resuspended in 1 ml of 1-ODE and rapidly injected into a flask containing 5 ml of ODE at 290 °C under N_2 on a Schlenk line. The reaction was monitored by UV-Vis and PL aliquots to determine the endpoint of growth, at which point the heating mantle was removed and the flask was placed into a silicone oil bath to rapidly cool down. For sample characterization, ODE was removed under vacuum distillation and the remaining QD solid was resuspended in a minimal amount of toluene inside a glovebox. Acetonitrile was added to precipitate the particles and centrifuged at 7500 rpm for 10 min. After removing the clear supernatant, the film of QDs was resuspended in toluene and purified by GPC. For ZnSeS growth, InP QDs were kept in the same flask following the hot-injection reaction in order to keep stoichiometry and volumes consistent.

F. Doped InP/ZnSeS core/shell synthesis

Shell growth was performed using a modified literature procedure from the study of Lee *et al.*[7] TOPSe and TOPS stock solutions (1M) were prepared by dissolving either 128 mg of sulfur powder (4 mmol) or 316 mg of selenium (4 mmol) in 4 ml of TOP. InP QDs that had previously been formed from clusters solutions were estimated to have 0.09 mmol of In^{3+}, assuming a 100% conversion of the cluster to the QD. The InP QD solution from before was heated to 220 °C. A solution of zinc stearate was prepared by suspending 570 mg (0.9 mmol) in 2 ml of ODE and then injected into the QDs. A blueshift was observed, corresponding to zinc surface passivation, which appeared to stop changing after 15 min. At this point, TOPSe (90 μl, 0.09 mmol) was added slowly over the course of 1 min and the reaction was allowed to equilibrate for 20 min. Next, TOPS (810 μl, 0.81 mmol) was added slowly over the course of 5 min and the reaction was allowed to equilibrate for 15 min. The temperature was then set to 300 °C and the PL was monitored until no further increases were measured (40 min following TOPS injection). The reaction was cooled to room temperature, and the 1-ODE was removed under vacuum distillation. The solid was resuspended in toluene and centrifuged to isolate the supernatant, which was then precipitated with acetonitrile. The precipitate was then resuspended in minimal toluene and purified by GPC.

SUPPLEMENTARY MATERIAL

Additional experimental details and data are provided in the supplementary material document accompanying this manuscript.

ACKNOWLEDGMENTS

This research was supported primarily by the U.S. National Science Foundation (NSF) through the UW Molecular Engineering Materials Center (MEMC), a Materials Research Science and Engineering Center (Grant No. DMR-1719797). M.R.F. received financial support from a Washington Research Foundation postdoctoral fellowship. N.P. and D.A.J. were supported in their efforts to study cluster nucleation and growth and QD surface chemistry by the National Science Foundation under Grant No. CHE-1552164. Part of this work was conducted at the Molecular Analysis Facility, a National Nanotechnology Coordinated Infrastructure site at the University of Washington which is supported in part by the National Science Foundation (Grant No. NNCI-1542101), the University of Washington, the Molecular Engineering and Sciences Institute, and the Clean Energy Institute. Part of this work was supported through a sponsored project agreement with Merck Group/EMD Performance Materials.

REFERENCES

[1] J. S. Steckel, J. Ho, C. Hamilton, J. Xi, C. Breen, W. Liu, P. Allen, and S. Coe-Sullivan, "Quantum dots: The ultimate down-conversion material for LCD displays," J. Soc. Inf. Disp. **23**(7), 294–305 (2015).
[2] E. Lee, C. K. Wang, J. Yurek, and R. Ma, "A new frontier for quantum dots in displays," Inf. Disp. **34**(6), 10–13 (2018).
[3] K. R. Reid, J. R. McBride, N. J. Freymeyer, L. B. Thal, and S. J. Rosenthal, "Chemical structure, ensemble and single-particle spectroscopy of thick-shell InP–ZnSe quantum dots," Nano Lett. **18**(2), 709–716 (2018).
[4] P. Ramasamy, K.-J. Ko, J.-W. Kang, and J.-S. Lee, "Two-step "seed-mediated" synthetic approach to colloidal indium phosphide quantum dots with high-purity photo- and electroluminescence," Chem. Mater. **30**(11), 3643–3647 (2018).
[5] F. Cao, S. Wang, F. Wang, Q. Wu, D. Zhao, and X. Yang, "A layer-by-layer growth strategy for large-size InP/ZnSe/ZnS core–shell quantum dots enabling high-efficiency light-emitting diodes," Chem. Mater. **30**(21), 8002–8007 (2018).
[6] Y. Kim, S. Ham, H. Jang, J. H. Min, H. Chung, J. Lee, D. Kim, and E. Jang, "Bright and uniform green light emitting InP/ZnSe/ZnS quantum dots for wide color gamut displays," ACS Appl. Nano Mater. **2**(3), 1496–1504 (2019).
[7] J. Lim, W. K. Bae, D. Lee, M. K. Nam, J. Jung, C. Lee, K. Char, and S. Lee, "InP@ZnSeS, core@composition gradient shell quantum dots with enhanced stability," Chem. Mater. **23**(20), 4459–4463 (2011).
[8] J. L. Stein, E. A. Mader, and B. M. Cossairt, "Luminescent InP quantum dots with tunable emission by post-synthetic modification with Lewis acids," J. Phys. Chem. Lett. **7**(7), 1315–1320 (2016).
[9] M. Rafipoor, D. Dupont, H. Tornatzky, M. D. Tessier, J. Maultzsch, Z. Hens, and H. Lange, "Strain engineering in InP/(Zn,Cd)Se core/shell quantum dots," Chem. Mater. **30**(13), 4393–4400 (2018).
[10] C. K. De, T. Routh, D. Roy, S. Mandal, and P. K. Mandal, "Highly photoluminescent InP based core alloy shell QDs from air-stable precursors: Excitation wavelength dependent photoluminescence quantum yield, photoluminescence decay dynamics, and single particle blinking dynamics," J. Phys. Chem. C **122**(1), 964–973 (2018).
[11] M. D. Tessier, D. Dupont, K. De Nolf, J. De Roo, and Z. Hens, "Economic and size-tunable synthesis of InP/ZnE (E = S, Se) colloidal quantum dots," Chem. Mater. **27**(13), 4893–4898 (2015).
[12] S. Koh, T. Eom, W. D. Kim, K. Lee, D. Lee, Y. K. Lee, H. Kim, W. K. Bae, and D. C. Lee, "Zinc–phosphorus complex working as an atomic valve for colloidal

growth of monodisperse indium phosphide quantum dots," Chem. Mater. **29**(15), 6346–6355 (2017).
[13]S. Kim, T. Kim, M. Kang, S. K. Kwak, T. W. Yoo, L. S. Park, I. Yang, S. Hwang, J. E. Lee, S. K. Kim *et al.*, "Highly luminescent InP/GaP/ZnS nanocrystals and their application to white light-emitting diodes," J. Am. Chem. Soc. **134**(8), 3804–3809 (2012).
[14]H. Zhang, N. Hu, Z. Zeng, Q. Lin, F. Zhang, A. Tang, Y. Jia, L. S. Li, H. Shen, F. Teng *et al.*, "High-efficiency green InP quantum dot-based electroluminescent device comprising thick-shell quantum dots," Adv. Opt. Mater. **7**(7), 1801602 (2019).
[15]K. D. Wegner, S. Pouget, W. L. Ling, M. Carrière, and P. Reiss, "Gallium – a versatile element for tuning the photoluminescence properties of InP quantum dots," Chem. Commun. **55**(11), 1663–1666 (2019).
[16]F. Pietra, N. Kirkwood, L. De Trizio, A. W. Hoekstra, L. Kleibergen, N. Renaud, R. Koole, P. Baesjou, L. Manna, and A. J. Houtepen, "Ga for Zn cation exchange allows for highly luminescent and photostable InZnP-based quantum dots," Chem. Mater. **29**(12), 5192–5199 (2017).
[17]D. C. Gary, S. E. Flowers, W. Kaminsky, A. Petrone, X. Li, and B. M. Cossairt, "Single-crystal and electronic structure of a 1.3 nm indium phosphide nanocluster," J. Am. Chem. Soc. **138**(5), 1510–1513 (2016).
[18]D. C. Gary, M. W. Terban, S. J. L. Billinge, and B. M. Cossairt, "Two-step nucleation and growth of InP quantum dots via magic-sized cluster intermediates," Chem. Mater. **27**(4), 1432–1441 (2015).
[19]M. R. Friedfeld, D. A. Johnson, and B. M. Cossairt, "Conversion of InP clusters to quantum dots," Inorg. Chem. **58**(1), 803–810 (2019).
[20]J. L. Stein, M. I. Steimle, M. W. Terban, A. Petrone, S. J. L. Billinge, X. Li, and B. M. Cossairt, "Cation exchange induced transformation of InP magic-sized clusters," Chem. Mater. **29**(18), 7984–7992 (2017).
[21]K. L. Orchard, A. J. P. White, M. S. P. Shaffer, and C. K. Williams, "Pentanuclear complexes for a series of alkylzinc carboxylates," Organometallics **28**(19), 5828–5832 (2009).
[22]B. A. Glassy and B. M. Cossairt, "Resolving the chemistry of Zn_3P_2 nanocrystal growth," Chem. Mater. **28**(17), 6374–6380 (2016).
[23]M. R. Kaluđerović, S. Gómez-Ruiz, B. Gallego, E. Hey-Hawkins, R. Paschke, and G. N. Kaluđerović, "Anticancer activity of dinuclear gallium(III) carboxylate complexes," Eur. J. Med. Chem. **45**(2), 519–525 (2010).
[24]A. Keys, T. J. Barbarich, S. G. Bott, and A. R. Barron, "Tert-butyl compounds of gallium," J. Chem. Soc., Dalton Trans. **2000**(4), 577–588.
[25]I. P. Stolarov, I. A. Yakushev, A. V. Churakov, N. V. Cherkashina, N. S. Smirnova, E. V. Khramov, Y. V. Zubavichus, V. N. Khrustalev, A. A. Markov, A. P. Klyagina *et al.*, "Heterometallic palladium(II)-indium(III) and -gallium(III) acetate-bridged complexes: Synthesis, structure, and catalytic performance in homogeneous alkyne and alkene hydrogenation," Inorg. Chem. **57**(18), 11482–11491 (2018).
[26]R. D. Shannon, "Revised effective ionic radii and systematic studies of interatomic distances in halides and chalcogenides," Acta Crystallogr., Sect. A: Found. Adv. **32**(5), 751–767 (1976).
[27]R. G. Pearson, "Absolute electronegativity and hardness: Application to inorganic chemistry," Inorg. Chem. **27**(4), 734–740 (1988).
[28]F. Pietra, L. De Trizio, A. W. Hoekstra, N. Renaud, M. Prato, F. C. Grozema, P. J. Baesjou, R. Koole, L. Manna, and A. J. Houtepen, "Tuning the lattice parameter of In_XZn_YP for highly luminescent lattice-matched core/shell quantum dots," ACS Nano **10**(4), 4754–4762 (2016).
[29]N. Kirkwood, J. O. V. Monchen, R. W. Crisp, G. Grimaldi, H. A. C. Bergstein, I. du Fossé, W. van der Stam, I. Infante, and A. J. Houtepen, "Finding and fixing traps in II–VI and III–V colloidal quantum dots: The importance of Z-type ligand passivation," J. Am. Chem. Soc. **140**(46), 15712–15723 (2018).
[30]P. Reiss, M. Protière, and L. Li, "Core/shell semiconductor nanocrystals," Small **5**(2), 154–168 (2009).
[31]D. C. Gary, A. Petrone, X. Li, and B. M. Cossairt, "Investigating the role of amine in InP nanocrystal synthesis: Destabilizing cluster intermediates by Z-type ligand displacement," Chem. Commun. **53**(1), 161–164 (2017).
[32]D. C. Gary and B. M. Cossairt, "Role of acid in precursor conversion during InP quantum dot synthesis," Chem. Mater. **25**(12), 2463–2469 (2013).